Investigating the Growth Process of Vertically Aligned Single-Walled Carbon Nanotubes Synthesized from Alcohol

Erik Einarsson, Rong Xiang, Kazuaki Ogura, Jun Okawa, Zhengyi Zhang, and Shigeo Maruyama

Dept. of Mechanical Engineering, The University of Tokyo, 7-3-1 Hongo, Bunkyo-ku, Tokyo, 113-8656, Japan

ABSTRACT

We have performed a systematic investigation of the influence of growth parameters on the synthesis of vertically aligned single-walled carbon nanotubes (VA-SWNTs) by the alcohol catalytic chemical vapor deposition (ACCVD) method. The growth process of the VA-SWNTs was monitored using an *in situ* optical absorbance technique and the effects of CVD temperature and ethanol pressure on the initial growth rate and the catalyst lifetime were investigated. We found that for a given CVD temperature, there is an optimum pressure at which VA-SWNT film growth is maximized, and this pressure increases with temperature. Below this optimum pressure, the growth reaction is first-order, with the arrival of ethanol to the catalyst being the rate-limiting step. The activation energy of the growth reaction was determined to be approximately 1.5 eV.

The root-growth mechanism of VA-SWNTs synthesized by the alcohol CVD method was also confirmed by a two-stage growth process. Following a short growth period using normal ethanol, ^{13}C -labeled ethanol was introduced to continue the growth. The location of the ^{13}C was determined from resonance Raman spectra, confirming the root-growth mechanism.

INTRODUCTION

Single-walled carbon nanotubes (SWNTs) have attracted much attention in various scientific fields due to their unique physical properties, which arise from their one-dimensional nature. Some of these properties, such as near-ballistic transport [1], nonlinear optical absorption [2,3] and high thermal conductivity [4-6] make SWNTs particularly well-suited for many potential applications. Many of these properties, however, are highly anisotropic, thus it is desirable to control the orientation of SWNTs during synthesis. Significant advancements in this area have been made in the past few years, particularly regarding the synthesis of vertically aligned (VA-) SWNTs [7-12]. These synthesis methods, however, depend on several parameters such as temperature, pressure, flow rate, etc., and the underlying mechanism is not yet well understood. Here we report some recent findings related to the growth mechanism of VA-SWNTs, particularly the effects of growth temperature and pressure in the alcohol catalytic chemical vapor deposition (ACCVD) method [13].

EXPERIMENT

The VA-SWNTs used in this study were synthesized on quartz substrates by the catalytic reaction between ethanol vapor and cobalt nanoparticles on the substrate surface. The catalyst nanoparticles were prepared [7,14] by dip-coating optically polished quartz substrates into two solutions. The first solution was molybdenum acetate, $(CH_3COO)_2Mo$, dissolved in ethanol (Mo content 0.01 wt%). After dip-coating, the substrate was baked in air at 400 °C for 5 min, and then dip-coated into a second solution containing cobalt acetate, $(CH_3COO)_2Co\text{-}4H_2O$, at the same concentration. Following this second dip-coat step, the substrate was again baked in air before placing in the CVD chamber. A diagram of the CVD system is shown in figure 1, and consists primarily of an electronic furnace, a quartz tube, and an oil-free scroll pump. Growth of the VA-SWNT film can be monitored in real-time by an *in situ* optical absorbance measurement [14], where a laser (488 nm) is incident normal to the dip-coated quartz substrate through a small opening (~4 mm dia.) in the CVD furnace. The laser passes through the substrate and the growing VA-SWNT film, and then through another small opening on the opposite side of the furnace, where its intensity is measured. The absorbance, which is proportional to the film thickness, is determined from the intensity attenuation described by the Beer-Lambert law. This *in situ* measurement was used to investigate the influence of pressure and temperature on VA-SWNT growth. This method was also used to monitor growth during a two-stage process, in which normal ethanol and isotope-labeled ^{13}C ethanol were introduced sequentially to determine the location of the catalyst nanoparticles during growth.

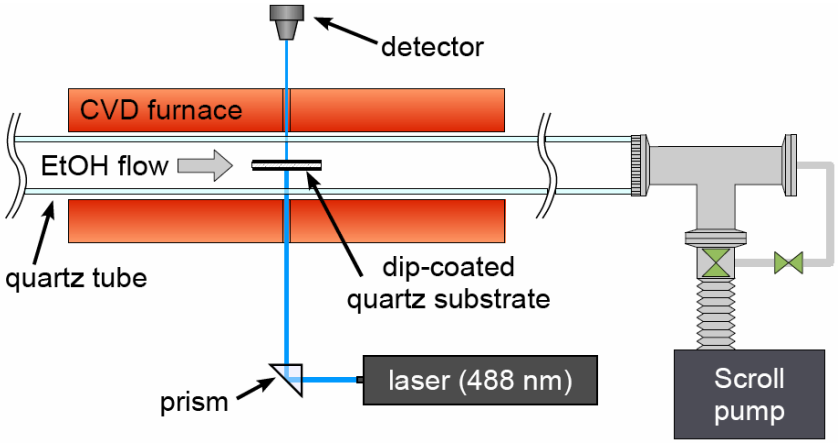

Figure 1. Schematic of the CVD furnace used for VA-SWNT synthesis. The *in situ* absorbance measurement setup is also shown.

DISCUSSION

Clarification of root-growth mechanism

We first describe a two-stage growth process [15] by which the VA-SWNT growth mechanism (root-growth or tip-growth) was clarified. Using the system shown in figure 1, ethanol vapor (99.5% pure) was introduced into the CVD chamber for approximately 90 sec, and growth was confirmed by an *in situ* optical absorbance measurement. The CVD chamber was then evacuated (~30 sec), and isotope-labeled ethanol ($^{13}CH_3{}^{13}CH_2OH$) was introduced. Subsequent growth from the ^{13}C ethanol was confirmed from the absorbance measurement.

An SEM image of the film cross-section is shown in figure 2a. The film thickness determined from absorbance is shown in figure 2b. The blue line represents growth from ^{12}C ethanol, and the red line from isotope-labeled ^{13}C ethanol. Since the two growth stages were separated by a short evacuation period, the VA-SWNTs in the vertically aligned film should consist of a purely ^{12}C segment approximately 7.5 µm thick, and a purely ^{13}C segment approximately 1.5 µm thick. Whether the latter is found at the top or the bottom of the VA-SWNT film will reveal whether the growth mechanism is root-growth or tip-growth. A diagram of the root-growth case is shown in the inset of figure 2b.

The location of the ^{13}C was determined from resonant Raman scattering spectra taken from the top and at various points along the height of the VA-SWNT film. Approximate locations of the measured spectra are shown on figure 2a. The G-band peak of the corresponding Raman spectra is shown in figure 2c. Since the Raman signal represents the excitation of a lattice vibration, the frequency of the Raman shift is related to the mass of the vibrating atoms in the lattice. The G-band peak in spectra 1 and 2 (figure 2c) is located at the usual position for ^{12}C (1592 cm^{-1}). Spectra 3 and 4 show the emergence of a secondary peak at 1530 cm^{-1}, indicating the border between the ^{12}C and ^{13}C segments. Spectrum 5, taken from the base of the film, shows only the new peak, the frequency of which is precisely at the expected location for ^{13}C, i.e. shifted by the square root of the relative atomic masses. These Raman spectra clearly show the ^{13}C, introduced at the end of growth, is located at the root of the film, thus the VA-SWNTs form by a root-growth process.

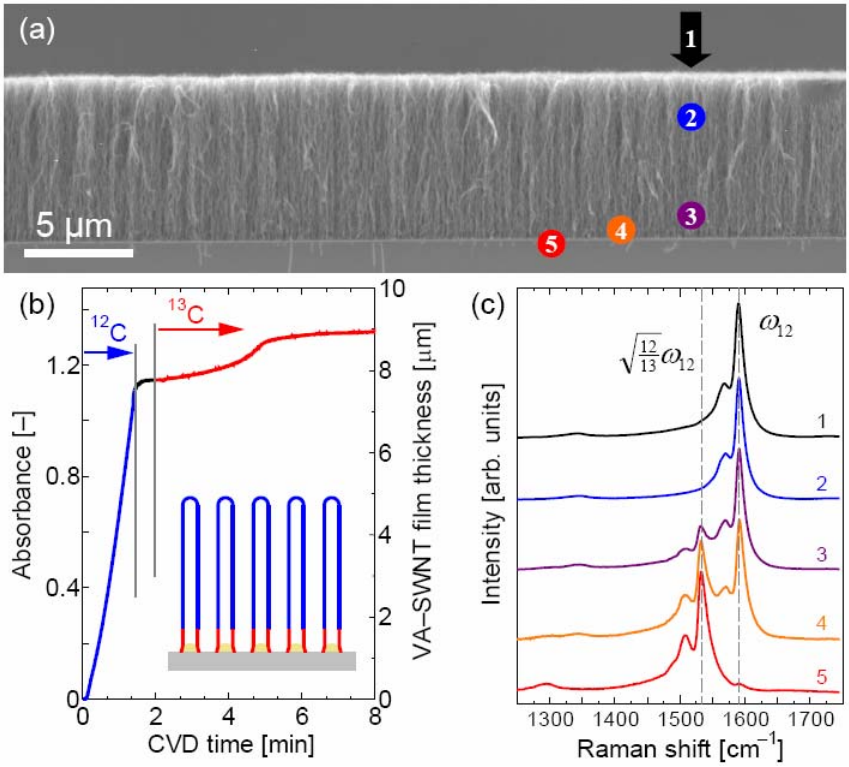

Figure 2. (a) SEM image of a VA-SWNT film cross section. (b) Two-stage growth profile of the VA-SWNT film in (a) synthesized from ^{12}C and ^{13}C. Inset shows the location of isotopes for the root-growth case. (c) Raman spectra taken from (a) at corresponding numbered locations. Change in the G-band shows ^{13}C is at root of VA-SWNT film, confirming root growth.

Influence of pressure and temperature on VA-SWNT growth

In this section we investigate the influence of CVD temperature and ethanol pressure on the growth dynamics of VA-SWNT films [16]. Figure 3 shows the effect of ethanol pressure on the maximum film thickness of VA-SWNTs synthesized at different temperatures. The plotted curves are only guides to show the trends in the data. We see there is some optimum pressure at which overall VA-SWNT growth is maximized. This pressure, P_{opt}, increases with higher CVD temperature.

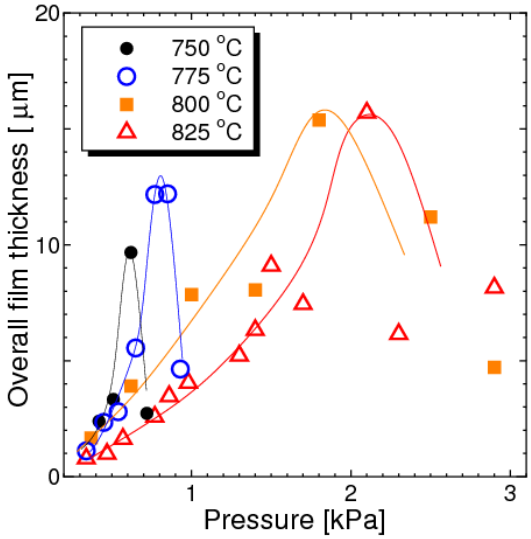

Figure 3. Overall VA-SWNT film thickness for different ethanol pressures and CVD temperatures. The lines show the trends in the data, revealing the optimum pressures.

The overall growth of the VA-SWNT films can be described in terms of two parameters [16], the initial growth rate, γ_0 [µm s^{-1}], and a reaction time constant (catalyst lifetime), τ [s]. The overall height L [µm] of the VA-SWNT film is described by the equation

$$L(t) = \gamma_0 \tau \left(1 - \exp \tfrac{-t}{\tau}\right). \qquad (1)$$

In order to gain some insight into the growth process, the data plotted in figure 3 are further decomposed into their γ_0 and τ components, obtained from iterative fitting of the *in situ* data using equation (1).

The pressure-temperature dependence of γ_0 is shown in Figure 4a. In this figure, it can be seen that below P_{opt} (approximately 1.8 kPa at 800 °C), the initial growth rate is proportional to the ethanol pressure. This indicates the synthesis reaction is first-order, with the arrival rate of ethanol at the catalyst nanoparticle being the rate-determining step. Above P_{opt}, however, the growth rate decreases, indicating a change in the overall synthesis reaction. Since there are few data in this higher pressure range it is unclear whether γ_0 will tend toward zero at still higher pressures or if it will plateau at some constant value.

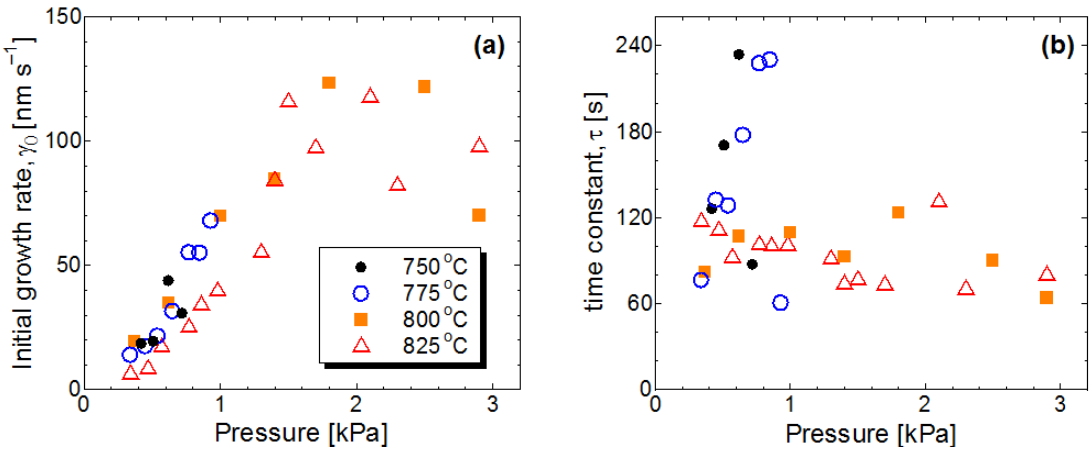

Figure 4. (a) Initial growth rates and (b) catalyst lifetimes for different CVD temperatures and ethanol pressures.

Figure 4b shows the effects of ethanol pressure on the catalyst lifetime, τ, for different CVD temperatures. Unlike the initial growth rate, there is no clear pressure-temperature dependence. At 800 and 825 °C, τ seems to fluctuate about a constant value, apparently independent of pressure. For lower temperatures (750 and 775 °C), however, τ has much more variation in a narrow pressure range. This suggests a change in the reaction mechanism between 775 and 800 °C, but the origin of this behavior is still being investigated.

As seen in figure 4a, for a given temperature there is some optimum pressure at which γ_0 is a maximum. Since γ_0 is directly related to the rate of the synthesis reaction occurring at the catalyst, we plot the temperature dependence of the growth rate as an Arrhenius plot in figure 5, using the values of γ_0 corresponding to each P_{opt}. The data are few, but by fitting these data with a line we can estimate the activation energy of the synthesis reaction, E_a, in the Arrhenius equation (inset). From this fitting we obtain a value of 1.5 eV. This is similar to the value of the activation energy reported for diffusion of carbon through a metal nanoparticle to the growth edge of a nanotube [17], but it is not yet clear if this is simply coincidence or if this is the primary step in the catalytic reaction.

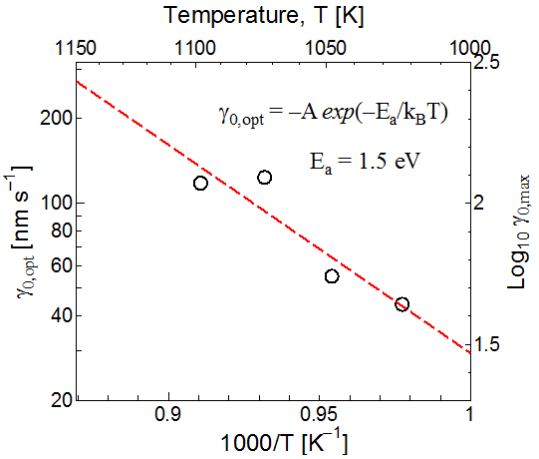

Figure 5. Arrhenius plot based on the initial growth rates corresponding to the optimum ethanol pressures at the four CVD temperatures investigated.

CONCLUSIONS

This study investigates the growth process of vertically aligned single-walled carbon nanotube (VA-SWNT) films synthesized from alcohol. Formation of the VA-SWNT films by a root-growth mechanism is confirmed by two-stage growth using isotope-labeled ethanol and identification of the ^{13}C location using resonance Raman spectroscopy. An *in situ* optical absorbance technique is used to determine the initial growth rate and catalyst lifetime for VA-SWNT films synthesized at different CVD temperatures and pressures. It was found that an optimum ethanol pressure exists, which depends on the growth temperature. Below this pressure, the growth reaction is first-order, and rate-limited by the arrival rate of ethanol at the catalyst.

ACKNOWLEDGMENTS

The present work was supported in part through the 21st Century COE Program, "Mechanical Systems Innovation," by the Ministry of Education, Culture, Sports, Science and Technology.

REFERENCES

1. N. Mingo and D. Broido, Phys. Rev. Lett. **95**, 096105 (2005).
2. M.F. Islam, D.E. Milkie, C.L. Kane, A.G. Yodh, and J.M. Kikkawa, Phys. Rev. Lett. **93**, 037404 (2004).
3. Y. Murakami, E. Einarsson, T. Edamura, and S. Maruyama, Phys. Rev. Lett. **94**, 087402 (2005).
4. S. Maruyama, Physica B **323**, 193 (2002).
5. C. Yu, L. Shi, Z. Yao, D. Li, and A. Majumdar, Nano Lett. **5**, 1842 (2005).
6. E. Pop, D. Mann, Q. Wang, K. Goodson, and H. Dai, Nano Lett. **6**, 96 (2006).
7. Y. Murakami, S. Chiashi, Y. Miyauchi, M. Hu, M. Ogura, T. Okubo, and S. Maruyama, Chem. Phys. Lett. **385**, 298 (2004).
8. K. Hata, D.N. Futaba, K. Mizuno, T. Namai, M. Yumura, and S. Iijima, Science **306**, 1362 (2004).
9. G. Zhong, T. Iwasaki, K. Honda, Y. Furukawa, I. Ohdomari, and H. Kawarada, Chem. Vap. Dep. 11, 127 (2005).
10. Y.-Q. Xu, E. Flor, M.J. Kim, H. Behrang, H. Schmidt, R.E. Smalley, and R.H. Hauge, J. Am. Chem. Soc. **128**, 6560 (2006).
11. L. Zhang, Y. Tan, and D.E. Resasco, Chem. Phys. Lett. **422**, 198 (2006).
12. S. Noda, H. Sugime, T. Osawa, T. Yoshiko, S. Chiashi, Y. Murakami, and S. Maruyama, Carbon **44**, 1414 (2006).
13. S. Maruyama, R. Kojima, Y. Miyauchi, S. Chiashi, and M. Kohno, Chem. Phys. Lett. **360**, 229 (2002).
14. S. Maruyama, E. Einarsson, Y. Murakami, and T. Edamura, Chem. Phys. Lett. **403**, 320 (2005).
15. R. Xiang, Z. Zhang, K. Ogura, J. Okawa, E. Einarsson, Y. Miyauchi, J. Shiomi, and S. Maruyama, submitted to Jpn. J. Appl. Phys.
16. E. Einarsson, Y. Murakami, M. Kadowaki, and S. Maruyama, submitted to Carbon.
17. O.A. Louchev, T. Laude, Y. Sato, and H. Kanda, J. Chem. Phys. **118**, 7622 (2003).